SELF-PRUNING Acts Synergistically with DIAGEOTROPICA to Guide Auxin Responses and Proper Growth Form[1]

Willian B. Silva,[a,2] Mateus H. Vicente,[b,2] Jessenia M. Robledo,[a,2] Diego S. Reartes,[b] Renata C. Ferrari,[c] Ricardo Bianchetti,[c] Wagner L. Araújo,[d] Luciano Freschi,[c] Lázaro E. P. Peres,[b] and Agustin Zsögön[a,3]

[a]Departamento de Biologia Vegetal, Universidade Federal de Viçosa, CEP 36570-900, Viçosa, MG, Brazil
[b]Laboratory of Hormonal Control of Plant Development, Departamento de Ciências Biológicas, Escola Superior de Agricultura Luiz de Queiroz, Universidade de São Paulo, CP 09, 13418-900, Piracicaba, SP, Brazil
[c]Instituto de Biociências, Universidade de São Paulo, CEP 05508-900, São Paulo, SP, Brazil
[d]Max-Planck Partner Group at the Departamento de Biologia Vegetal, Universidade Federal de Viçosa, 36570-900, Viçosa, MG, Brazil

ORCID IDs: 0000-0003-4885-8404 (M.H.V.); 0000-0001-6205-9196 (J.M.R.); 0000-0002-8117-0380 (D.S.R.); 0000-0002-9497-8442 (R.C.F.); 0000-0001-8739-5460 (R.B.); 0000-0002-4796-2616 (W.L.A.); 0000-0002-0737-3438 (L.F.); 0000-0002-8761-5934 (L.E.P.P.); 0000-0001-7828-7425 (A.Z.).

The *SELF PRUNING* (*SP*) gene is a key regulator of growth habit in tomato (*Solanum lycopersicum*). It is an ortholog of *TERMINAL FLOWER1*, a phosphatidylethanolamine-binding protein with antiflorigenic activity in Arabidopsis (*Arabidopsis thaliana*). A spontaneous loss-of-function mutation (*sp*) has been bred into several industrial tomato cultivars, as it produces a suite of pleiotropic effects that are favorable for mechanical harvesting, including determinate growth habit, short plant stature, and simultaneous fruit ripening. However, the physiological basis for these phenotypic differences has not been thoroughly explained. Here, we show that the *sp* mutation alters polar auxin transport as well as auxin responses, such as gravitropic curvature and elongation of excised hypocotyl segments. We also demonstrate that free auxin levels and auxin-regulated gene expression patterns are altered in *sp* mutants. Furthermore, *diageotropica*, a mutation in a gene encoding a cyclophilin A protein, appears to confer epistatic effects with *sp*. Our results indicate that SP affects the tomato growth habit at least in part by influencing auxin transport and responsiveness. These findings suggest potential novel targets that could be manipulated for controlling plant growth habit and improving productivity.

Shoot architecture is a key agricultural trait determined mainly by side branching, internode elongation, and shoot determinacy (Wang and Li, 2008). Each of these parameters is an active research area where considerable theoretical and applied knowledge has been gained over the last decade. Shoot determinacy is a domestication trait found in several crop species, such as soybean (*Glycine max*), common bean (*Phaseolus vulgaris*), and tomato (*Solanum lycopersicum*; Pnueli et al., 1998; Tian et al., 2010; Repinski et al., 2012). Shoot determinacy is notably important for tomato, which is a perennial species cultivated as an annual crop. Wild tomatoes display indeterminate growth, resulting from a sequential addition of modules (sympodial units) formed by three leaves and an inflorescence. Sympodial growth starts in tomato when the vegetative apical meristem is converted into an inflorescence meristem after a series of eight to 12 internodes with leaves (Samach and Lotan, 2007). Vegetative growth, however, continues vigorously at the top-most axillary meristem, displacing the inflorescence to the side and producing a new sympodial unit with three leaves and an inflorescence. This process is iterated indefinitely by a concatenation of stacked sympodial units. However,

[1] This work was supported by funding from the Agency for the Support and Evaluation of Graduate Education (CAPES-Brazil), the National Council for Scientific and Technological Development (CNPq-Brazil), the Foundation for Research Assistance of the São Paulo State (FAPESP-Brazil), and the Foundation for Research Assistance of the Minas Gerais State (FAPEMIG-Brazil). We thank CAPES for studentships granted to J.M.R., W.B.S., and D.S.R. FAPESP provided grants for M.H.V. (2016/05566-0), L.F. (2013/18056-2), L.E.P.P. (2015/50220-2), and A.Z. (2013/11541-2). W.L.A. and L.E.P.P. also acknowledge grants from CNPq (grant 307040/2014-3 to L.E.P.P.). We thank Cássia Figueiredo (ESALQ, USP) for help preparing and analyzing microscopy samples. We thank Biomatters, Ltd. (Auckland, New Zealand), for the kind gift of a Geneious R9 license.

[2] These authors contributed equally to the article.
[3] Address correspondence to agustin.zsogon@ufv.br.

The author responsible for distribution of materials integral to the findings presented in this article in accordance with the policy described in the Instructions for Authors (www.plantphysiol.org) is: Agustin Zsögön (agustin.zsogon@ufv.br).

W.B.S., M.H.V., and J.M.R. generated the plant material and conducted experiments; W.B.S., M.H.V., J.M.R., D.S.R., L.F., R.C.F., and R.B. conducted experiments and prepared figures and/or tables; L.F. and W.L.A. designed experiments, contributed reagents/materials/analysis tools, and reviewed drafts of the article; A.Z. and L.E.P.P. conceived and designed the experiments, analyzed the data, and wrote the article.

www.plantphysiol.org/cgi/doi/10.1104/pp.18.00038

a spontaneous recessive mutant with a compact, bushy growth habit and a reduced number of leaves in successive sympodial units was discovered in 1914 (Yeager, 1927; MacArthur, 1934). It was later shown that the mutation is a single-nucleotide substitution in the *SELF-PRUNING* (*SP*) gene (Pnueli et al., 1998), which shares sequence similarity with phosphatidylethanolamine-binding proteins (PEBPs), a group of mammalian polypeptides involved in cell signaling (Hengst et al., 2001; Kroslak et al., 2001). Breeding the *SP* mutation into industrial tomato cultivars was instrumental in the advent of mechanical harvest (Rick, 1978; Stevens and Rick, 1986). The loss-of-function *sp* mutant exhibits a determinate growth habit, as opposed to the indeterminate growth habit of wild-type tomatoes. The determinate growth habit occurs via a progressively reduced number of leaves per sympodium until termination in two consecutive inflorescences that top the vertical growth of the plant (Samach and Lotan, 2007). Hence, this phenotype leads to simultaneous fruit ripening, allowing mechanical harvest in field-grown processing tomatoes (Stevens and Rick, 1986).

SP belongs to the *CETS* gene family, which comprises *CENTRORADIALIS* (*CEN*) and *TERMINAL FLOWER1* (*TFL1*) of *Antirrhinum* spp. and Arabidopsis (*Arabidopsis thaliana*), respectively (Wickland and Hanzawa, 2015). *SINGLE FLOWER TRUSS* (*SFT*)/*SP3D*, a homolog of *FLOWERING LOCUS T* and *HEADING DATE3A* in Arabidopsis and rice (*Oryza sativa*), respectively, is another *CETS* gene involved in controlling tomato growth habit (Alvarez et al., 1992; Kojima et al., 2002). Unlike *sp* mutants, which do not affect flowering time, tomato *sft* loss-of-function mutants are late flowering and show a disruption in sympodial growth pattern. These mutants produce a single and highly vegetative inflorescence as well as alternating solitary flowers and leaves (Molinero-Rosales et al., 2004). The final phenotypic outcome produced by SP and SFT depends on their local ratio, with the former maintaining meristems in an indeterminate state and the latter promoting the transition to flowering (Park et al., 2014). Heterozygous *sft* mutants in a homozygous *sp* mutant background display yield heterosis in tomato (Krieger et al., 2010). Hence, the *SP*/*SFT* genetic module has been proposed as a target to increase crop yield via changes in plant architecture (McGarry and Ayre, 2012; Zsögön et al., 2017). It also has been suggested that *SP* function could be linked to auxin (Pnueli et al., 2001), a hormone with strong effects on plant morphogenesis (Berleth and Sachs, 2001).

Auxin is a key controller of plant development; however, its role in the regulation of plant growth habit is still unclear. An aspect that sets auxin apart from other plant hormones is the relatively well-understood nature of its transport through the plant body (Friml, 2003; Petrášek and Friml, 2009). Polar auxin transport (PAT), which occurs basipetally from the apical meristem, is crucial for the distribution of auxin within plant tissues (Rubery and Sheldrake, 1974; Sheldrake, 1974). PAT works as an organizer of apical-basal polarity in the plant body (Friml et al., 2006), thus controlling a multiplicity of developmental processes (Reinhardt et al., 2003; Blilou et al., 2005; Scarpella et al., 2006).

It was shown recently that DIAGEOTROPICA (DGT) affects PAT in tomato (Ivanchenko et al., 2015). DGT is a cyclophilin A protein with peptidyl-prolyl trans/cis-isomerase (PPIase) enzymatic activity (Takahashi et al., 1989; Oh et al., 2006). Cyclophilins catalyze not only rate-limiting steps in the protein-folding pathway but also can participate in the folding process as molecular chaperones (Kumari et al., 2013). DGT function is highly conserved across plant taxa (Lavy et al., 2012). In tomato, some of the most significant phenotypic defects caused by the lack of functional DGT protein are horizontal shoot growth, thin stems, altered secondary vascular differentiation, and roots lacking lateral branches (Zobel, 1973; Muday et al., 1995; Coenen et al., 2003). Here, we investigated whether *SP* affects auxin responses by itself and in combination with *DGT*. We produced four combinations of functional and loss-of-function mutant alleles of *SP* and *DGT* (i.e. *SP DGT*, *SP dgt*, *sp DGT*, and *sp dgt*) in a single tomato genetic background (cv Micro-Tom [MT]) and assessed a series of physiological responses to auxin. We found that free auxin levels, PAT, and gravitropic curvature of the shoot apex are all altered by *SP*. Our results further show that *SP* and *DGT* reciprocally affect *AUXIN/INDOLE-3-ACETIC ACID INDUCIBLE* (*Aux/IAA*) and *AUXIN RESPONSE FACTOR* (*ARF*) transcript abundances at the sympodial meristem, the key niche of *SP* function in growth habit.

RESULTS

Comparison of the four combinations of homozygous wild-type and mutant lines for *SP* and *DGT* (i.e. *SP DGT*, *SP dgt*, *sp DGT*, and *sp dgt*) showed that growth habit was affected solely by *SP* and not by *DGT* (Fig. 1). Regardless of their *DGT* or *dgt* allele, *SP* plants showed indeterminate growth whereas *sp* mutants were always determinate (Fig. 1). Time to flowering, however, was affected by both genes in a combinatorial fashion: *dgt* plants flowered late, independently of the *SP* allele (Fig. 1). The *sp DGT* genotype showed consistently precocious flowering, and this was confirmed in an independent experiment by analysis of the rate of shoot apical meristem maturation (Supplemental Fig. S1). The number of leaves to the first inflorescence also was affected by the combination of alleles (Fig. 1), albeit not reflecting the time to flowering. The *dgt* mutant produced more leaves before flowering, but this effect was abolished in the double mutant *sp dgt*. Regardless of their *SP* allele, *dgt* mutants exhibited markedly reduced transcript abundance of the flowering inducer *SFT* compared with *DGT* plants (Fig. 1), which fits with the delayed flowering in these mutants in both *SP* and *sp* backgrounds (Fig. 1).

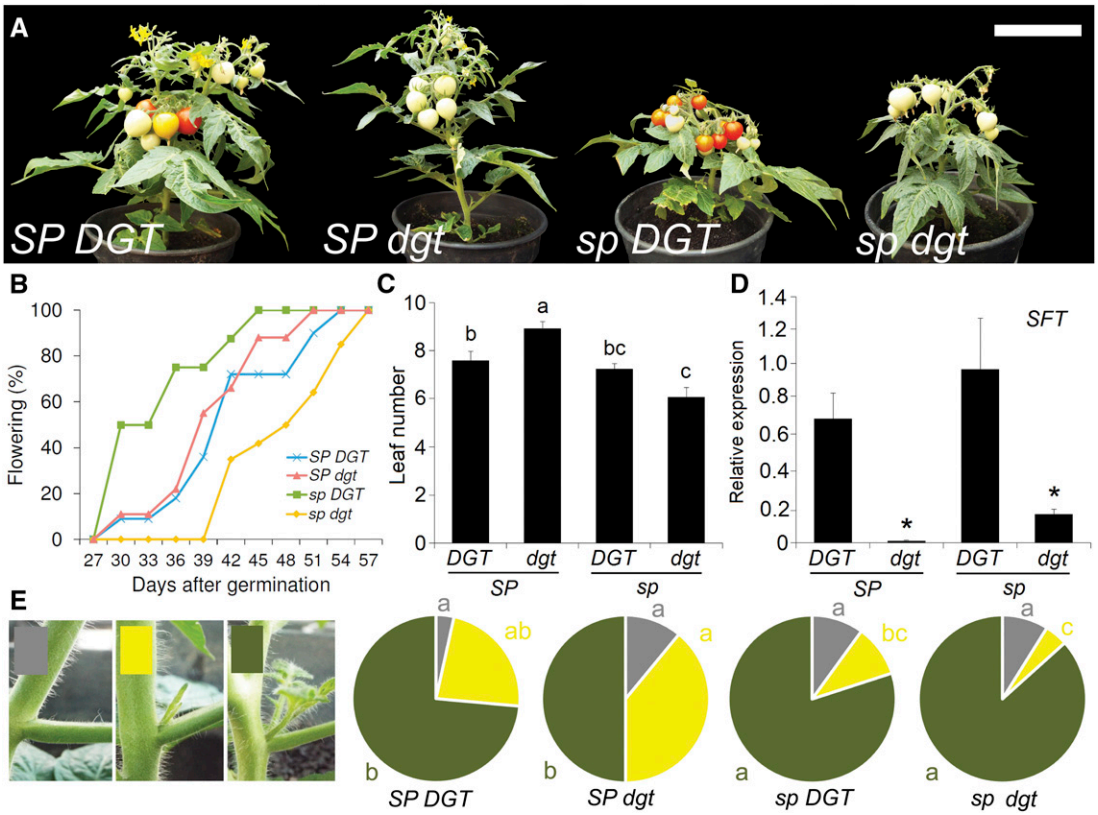

Figure 1. Additive phenotype of the *sp* and *dgt* mutations in tomato cv MT. A, Representative plants of *SP DGT*, *SP dgt*, *sp DGT* (cv MT), and *sp dgt* at 90 d after germination (dag). Note the simultaneous fruit ripening in *sp* compared with *SP*, a well-known effect of the *sp* mutation. The *dgt* mutation delays fruit ripening (at least in part due to its late flowering, as indicated in B) in either genetic background. Bar = 5 cm. B, Chronological time to flowering in *sp* and *dgt* mutants. The percentage of plants ($n = 15$) with at least one open flower is shown. The cv MT (*sp DGT*) plants flower earlier than the wild-type plants (*SP DGT*), whereas *dgt* mutants are late flowering. C, Developmental time to flowering in *sp* and *dgt* mutants. The number of leaves produced before the first inflorescence was reduced in *sp DGT* (cv MT) and increased in genotypes carrying the functional allele of *SP*. Letters indicate statistically significant differences (Dunn's multiple comparisons test, $P < 0.05$). D, *sp* and *dgt* alter the expression of the flowering inducer *SFT*. The *dgt* mutation leads to lower *SFT* expression and, thus, delays flowering. A minor influence from *SP* reducing *SFT* levels also is noticeable. Asterisks indicate statistically significant differences from the wild-type *SP DGT* (Student's *t* test, $P < 0.05$). E, Effects of *sp* and *dgt* on side branching. Pie charts depict the distribution of side branches in each genotype at 60 dag ($n = 15$ plants). Gray denotes absence of an axillary bud, yellow denotes a visible bud (greater than 1 cm), and dark green denotes a full branch (with one or multiple leaves). Letters indicate statistically significant differences (Dunn's multiple comparisons test, $P < 0.05$).

The tomato cv MT harbors a mutation in *DWARF* (*D*), a gene coding for a key enzyme in the brassinosteroid biosynthesis pathway (Bishop et al., 1999). Since brassinosteroids are known to influence the flowering induction network (Domagalska et al., 2010; Li et al., 2010), we ascertained whether *D* could be influencing the effects of *SP* on flowering time. Using a near-isogenic MT line harboring the functional *D* allele (Carvalho et al., 2011), we constructed four allelic combinations of *SP* and *D* (i.e. *SP D*, *SP d*, *sp D*, and *sp d*; Supplemental Fig. S2) and assessed their flowering time. The results show an effect of *D* on flowering time (Supplemental Fig. S2) but not on the number of leaves produced to the first inflorescence, which was again reduced exclusively by the presence of the *sp* mutant allele (Supplemental Fig. S2). Axillary branching was affected mainly by the *SP* gene, which led to reduced bud outgrowth in plants carrying the wild-type allele; the *dgt* mutation, however, exacerbated this repressive effect (Fig. 1). *sp* mutants, on the other hand, branched more profusely when combined with *dgt* than when combined with *DGT* (Fig. 1). Thus, *dgt* can enhance apical dominance or increase branching, depending on the presence or absence of a functional *SP* allele, respectively. The number of leaves on the primary shoot was increased by *SP*, regardless of the *DGT* allele (Table I). Plant height was additively controlled by both genes, whereas no difference between genotypes was found in the length of the fourth internode or the leaf insertion angle (Table I). Stem diameter was increased by functional *DGT*, irrespective of the *SP* allele (Table I). The number of inflorescences was determined synergistically

Table I. *Parameters that define growth habit*

Parameters are as follows: number of leaves on the primary shoot (number of leaves up to the first inflorescence); height of the primary shoot (cm); internode length (cm); leaf insertion angle (°); diameter of the stem (mm); number of flowers per inflorescence and number of inflorescences. Measurements were performed at 60 dag. Data are means ± SE (n = 10 plants). Different letters indicate statistically significant differences (Tukey's test, $P < 0.05$) among genotypes.

Parameters	*SP DGT*	*SP dgt*	*sp DGT*	*sp dgt*
No. of leaves on the primary shoot	9.00 ± 0.36 a	9.09 ± 0.28 a	7.50 ± 0.48 b	7.67 ± 0.58 b
Height of the main shoot	17.45 ± 0.79 a	12.74 ± 0.61 b	13.45 ± 0.49 b	10.70 ± 1.07 b
Length of the fourth internode	1.08 ± 0.12 a	1.11 ± 0.07 a	1.28 ± 0.13 a	1.22 ± 0.22 a
Leaf insertion angle	74.81 ± 3.41 a	74.87 ± 3.26 a	73.01 ± 4.38 a	63.54 ± 5.22 a
Stem diameter	5.46 ± 0.26 a	4.36 ± 0.12 a,b	5.36 ± 0.21 a	4.45 ± 0.1 b
Flowers per inflorescence	7.00 ± 0.71 b	7.80 ± 0.45 a	7.00 ± 0.00 b	7.00 ± 0.5 b
No. of inflorescences	12.4 ± 1.14 a	9.20 ± 1.30 b	7.40 ± 0.89 b	8.80 ± 1.48 b

by both genes, whereby the pairing of functional *SP* and *DGT* led to an increased number compared with all other allele combinations (Table I).

Next, the endogenous levels of free indolyl-3-acetic acid (IAA), which is the most abundant auxin in plants (Bartel and Fink, 1995), was determined in three sections of tomato seedlings: leaves plus cotyledons, hypocotyls, and roots (Fig. 2). In leaves plus cotyledons, IAA concentration was more than 2 times higher in the *sp dgt* double mutant than in the other three genotypes (Fig. 2). In the hypocotyl tissues, *SP DGT* seedlings had the lowest free IAA content, the *sp* and *dgt* single mutants had intermediate levels, and the double mutant (*sp dgt*) exhibited the highest IAA levels (Fig. 2). Although root IAA levels were clearly higher than in the other hypocotyl regions analyzed, no statistically significant differences in root IAA content were observed between the four genotypes (Fig. 2).

To understand the variation in endogenous free IAA levels within the seedling tissues and among the four genotypes, we next quantified PAT in hypocotyl segments. PAT was highest in *SP DGT*, intermediate in *sp* and *dgt* single mutants, and lowest in the double mutant (Fig. 3). This indicates that both *sp* and *dgt* alleles reduce PAT and that their effects are additive. As PAT and auxin concentration are known to influence vascular patterning (Scarpella, 2017), we also analyzed xylem anatomy in cross sections of stems in adult plants (Fig. 3). Quantification of xylem vessel density and mean vessel size revealed an antagonistic relationship

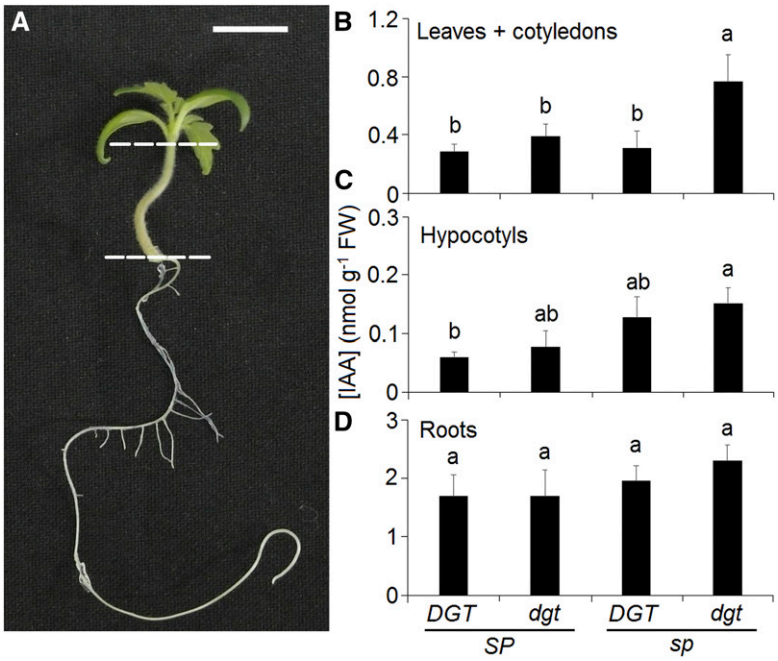

Figure 2. Auxin levels in tomato seedlings are affected synergistically by the *sp* and *dgt* mutations. A, Representative 7-d-old seedling showing the dissection points for auxin quantitation (bar = 1 cm). B to D, Free IAA levels in leaves + cotyledons (B), hypocotyls (C), and roots (D). Data are means ± SE (n = 10). Different letters indicate statistically significant differences (Tukey's test, $P < 0.05$) among genotypes. FW, Fresh weight.

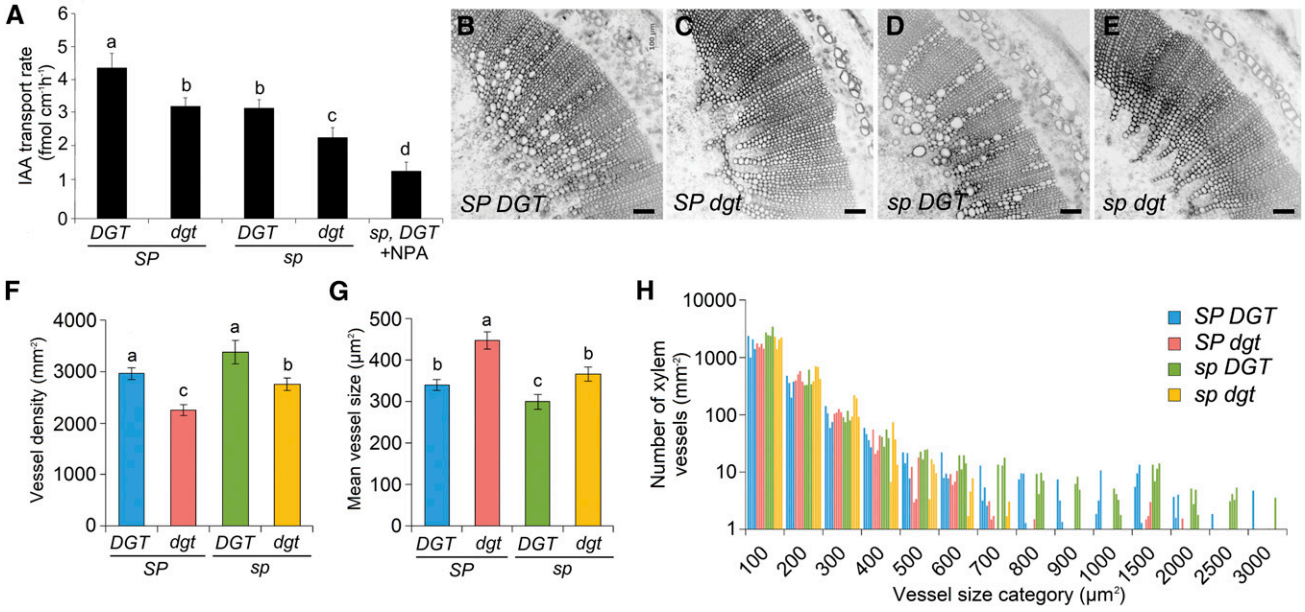

Figure 3. A, The *sp* mutation exacerbates defective PAT in hypocotyls caused by *dgt*. Basipetal [^{3}H]IAA transport is shown in 10-mm hypocotyl sections of the wild type (*SP DGT*), *SP dgt*, *sp DGT* (cv MT; also the negative control treated with 1-*N*-naphthylphthalamic acid [NPA]), and double mutant *sp dgt* roots. Data are means ± SE (n = 10). Letters indicate statistically significant differences between treatments (Tukey's test, $P < 0.05$). B to E, Vascular patterning in *sp* and *dgt* stems. Cross sections of the fifth internode taken at 45 dag are shown. Bars = 100 μm. F and G, Vessel density (F) and mean vessel size (G) in *sp* and *dgt* stems. Letters indicate significant differences ($P < 0.05$, ANOVA and Tukey's test). H, Vessel size distribution in the xylem of *sp* and *dgt* mutants. The *x* axis shows the upper values of cross-sectional area for each vessel size category. The bars within each category represent a single individual plant (n = 4 per genotype).

between *SP* and *DGT*. Whereas *SP* tends to reduce vessel density and increase their size, *DGT* increases vessel density with concomitantly lower vessel sizes (Fig. 3). These results, however, obscure a more complex pattern, which is revealed when analyzing the vessel size distributions. The functional *DGT* allele increased the incidence of larger vessels (greater than 800 μm^2 cross-sectional area), particularly in *sp* mutant plants (Fig. 3). Another physiological response affected by PAT is negative gravitropism of the shoot (Morita,

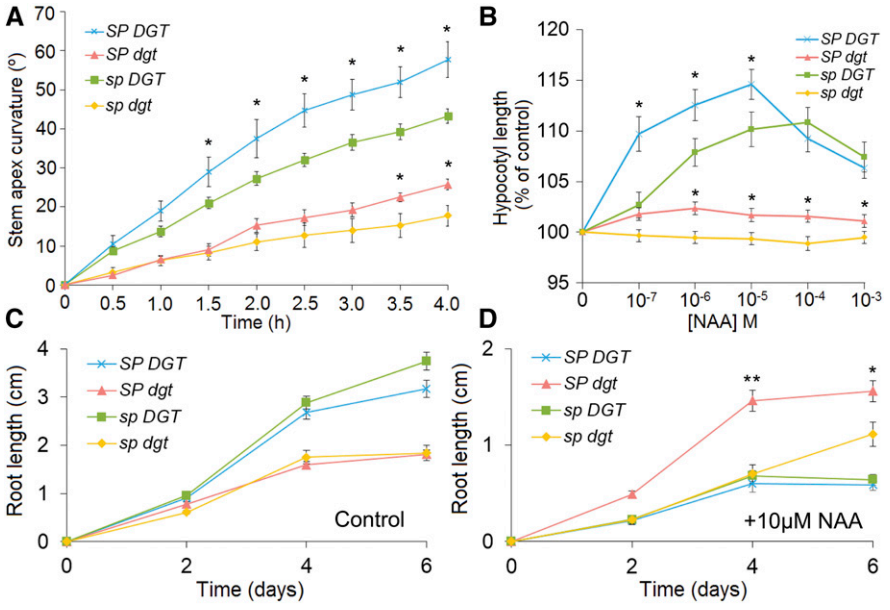

Figure 4. Impact of the *sp* mutation on auxin responses in planta. A, Kinetics of the gravitropic response in the shoot. Shoot angle is shown after placing plants horizontally at time point 0 (n = 5). B, Elongation of excised hypocotyls in response to naphthaleneacetic acid (NAA). Six-millimeter hypocotyl sections were incubated in the indicated NAA concentration for 24 h before measurement (n = 15). C and D, Time course of in vitro root elongation of seedlings in control and 10 μM NAA-containing Murashige and Skoog (MS) medium (n = 25). In all graphs, error bars indicate SE and asterisks indicate statistically significant differences between *SP* and *sp* plants harboring the same *DGT* allele (*, $P \leq 0.05$ and **, $P \leq 0.01$, Student's t test).

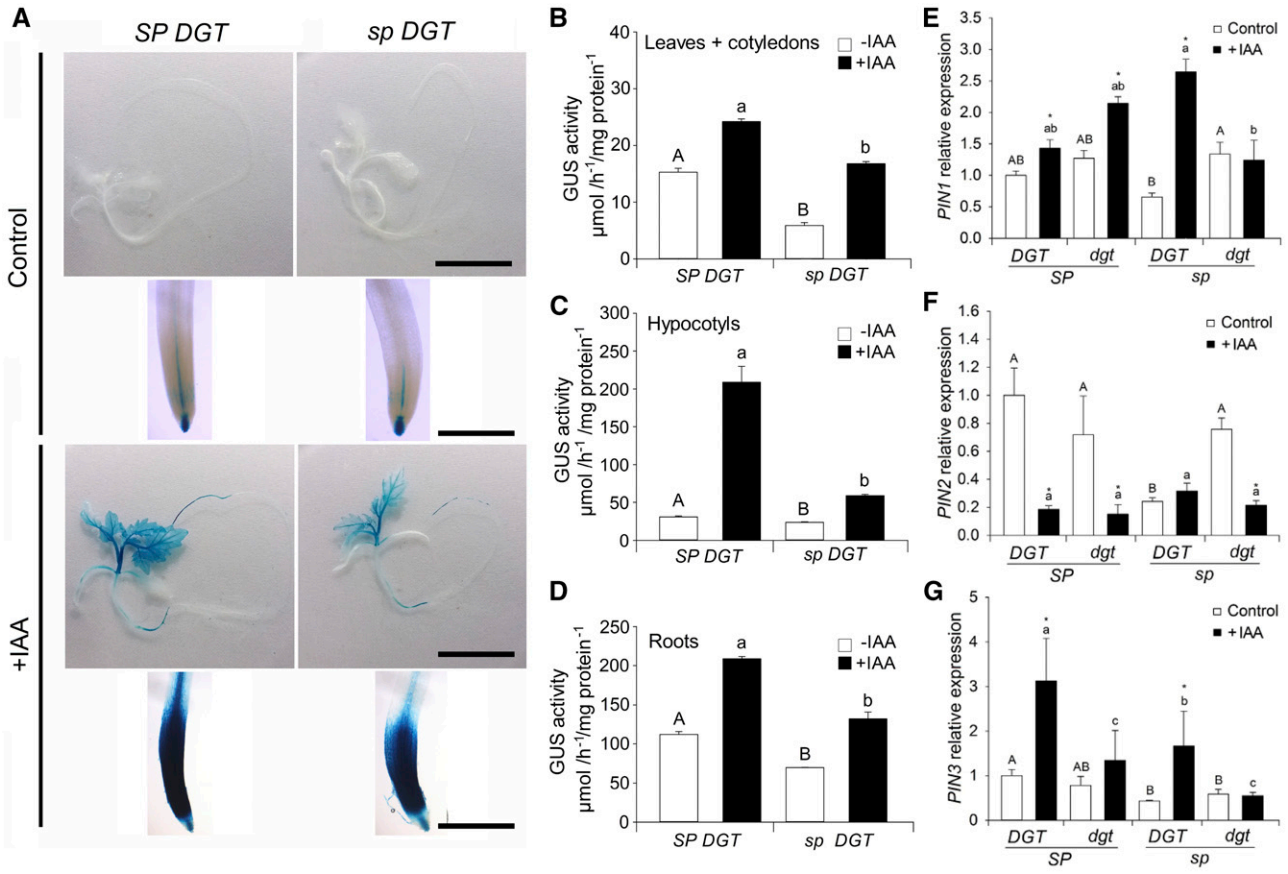

Figure 5. Effects of *SP* on the auxin signaling and transport machinery in planta. A, Expression of the GUS reporter driven by the auxin-inducible *DR5* promoter. Representative wild-type (*SP*) and mutant (*sp*) seedlings (bars = 2 cm) and their root tips (bars = 250 μm) are shown in the absence or presence of exogenous auxin (20 μM IAA, 3 h) at 15 dag. B to D, Fluorimetric quantification of GUS precipitate. Seedlings were sampled at 15 dag, after treatment with exogenous auxin (20 μM IAA, 3 h) or mock solution. Values are means ± SE ($n = 4$). Letters indicate significant differences between genotypes within the same treatment ($P < 0.05$, ANOVA and Tukey's test). E to G, Relative gene expression of *PIN* transporters in roots. Letters indicate significant differences between genotypes within the same treatment ($P < 0.05$, ANOVA and Tukey's test).

2010). The kinetics of gravitropic curvature in seedling shoots was affected by both *SP* and *DGT* (Fig. 4). Loss of *SP* function decreased the gravitropic response in both *DGT* and *dgt* backgrounds. Hypocotyl elongation in response to exogenous auxin and in vitro rhizogenesis from cotyledon explants are assays to determine auxin sensitivity (Cary et al., 2001). The *dgt* mutation considerably reduces hypocotyl responsivity to auxin in all concentrations, as described previously (Kelly and Bradford, 1986; Rice and Lomax, 2000). The functional *SP* allele increased hypocotyl elongation in the *DGT* background and also exerted a significant compensatory effect on the elongation response in the *dgt* mutant (Fig. 4). In the in vitro root regeneration assay, as expected, root formation was reduced in *dgt* mutants (Coenen and Lomax, 1998) but also in *sp* compared with *SP* in the presence of a functional *DGT* allele (Supplemental Fig. S3).

Histochemical analysis of *DR5* promoter activity revealed no discernible staining difference in both *SP* and *sp* seedlings incubated in water, although roots of the *sp* mutant showed a shorter trace of GUS precipitate in the vascular cylinder (Fig. 5). Exogenous IAA, however, strongly induced GUS expression in *SP* compared with *sp* plants, which was evident both in seedlings and in root tips and confirmed by fluorimetric GUS quantitation (Fig. 5). Fainter GUS staining was observed for both auxin-treated and untreated roots in the *dgt* mutant (Supplemental Fig. S4). As PIN-FORMED (PIN) auxin efflux transporters are key players determining auxin distribution in plants, we quantified the relative expression of the *PIN1*, *PIN2*, and *PIN3* genes in roots with or without prior auxin incubation. Auxin treatment induced *PIN1* and *PIN3* expression in all genotypes, except in the *sp dgt* double mutant (Fig. 5). *PIN2* expression was reduced by auxin incubation in *SP DGT*, *SP dgt*, and *sp dgt* but not in *sp DGT* (i.e. cv MT), where a low basal level of expression was observed for all three genes.

Finally, we determined whether auxin affects *SP* at the transcriptional level, as suggested by the presence

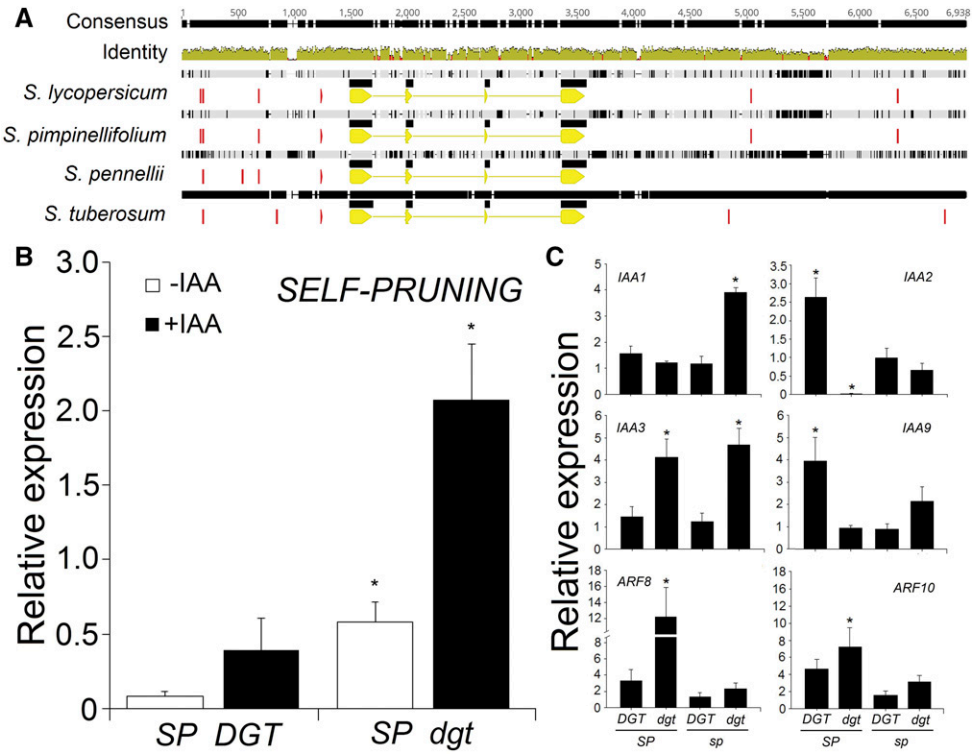

Figure 6. *SP* and auxin signaling gene expression is altered by the *dgt* mutation. A, Genomic structures of the *SP* gene in solanaceous species: tomato, its wild relatives *Solanum pimpinellifolium* and *Solanum pennellii*, and potato (*Solanum tuberosum*). The coding sequence is indicated in yellow (exons, thick bars; introns, thin bars). Red blocks indicate the presence of a conserved or degenerate auxin-response element (AuxRE), TGTCNC. B and C, Relative transcript accumulation of *SP* (B) and auxin signaling genes (C) in sympodial meristems. Tissues were sampled from 10-d-old plants 24 h after 10 μM IAA or mock spray. Asterisks indicate significant differences with respect to the wild-type *SP DGT* ($P < 0.05$, Student's *t* test).

of auxin-response elements (TGTCTC and the degenerate version, TGTCNC; Ulmasov et al., 1995) in the 3′ and 5′ flanking regions of the *SP* gene in tomato and related Solanaceae species (Fig. 6). Analyzing *SP* mRNA levels in seedlings of *SP DGT* and *sp DGT* plants sprayed with IAA or a mock solution revealed that *SP* expression was induced by IAA treatment in both genotypes. Importantly, *SP* transcript levels were significantly higher (Student's *t* test, $P < 0.05$) in *dgt* mutant plants than in wild-type *DGT*, both in IAA-treated and control seedlings (Fig. 6). We further assessed the effect of *SP* and *DGT* on the mRNA levels of key players in the auxin signaling cascades, including some members of the *ARF* and *Aux/IAA* gene families, which were chosen by their high auxin inducibility (Audran-Delalande et al., 2012). *SP* and *DGT* had combinatorial effects on the expression levels of *IAA1*, *IAA2*, *IAA9*, *ARF8*, and *ARF10*, whereas functional *DGT* decreased the expression of *IAA3* (Fig. 6).

DISCUSSION

Impact of SP Alleles, and Their Interaction with Auxin, in the Control of Shoot Architecture

Although it has been demonstrated previously that the *sp* mutation does not alter tomato flowering time or the number of leaves before termination of the shoot (Pnueli et al., 1998; Shalit et al., 2009), *SP* orthologs vary in this respect depending on the species. Flowering time is not affected in *cen* mutants in *Antirrhinum* spp. (Bradley et al., 1996), whereas Arabidopsis *tfl1* mutants flower earlier and *TFL1* overexpression delays flowering by preventing the meristem transition from vegetative to floral (Ratcliffe et al., 1998). In soybean, where large intraspecific variation exists in time to flowering, association mapping recently linked this important agronomic trait to the *Dt1* locus, a *CEN/TFL1/SP* ortholog (Zhang et al., 2015). Comparison of determinate and indeterminate near-isogenic soybean lines consistently showed earlier flowering in the former across different locations and planting seasons (Ouattara and Weaver, 1994). Our data show that loss of *SP* function (*sp* allele) leads to slightly but consistently earlier flowering in tomato, measured either in dag or the reduction of the number of nodes before the first inflorescence. Using a near-isogenic line harboring the wild-type *D* allele, which codes for a brassinosteroid biosynthesis gene (Martí et al., 2006), we demonstrate that this effect is not related to reduced brassinosteroid levels in cv MT. This is in agreement with the observation that the phenotypes of the *sp* and *dgt* individual mutants in the cv MT background closely resemble those published for the same mutations in other tomato cultivars (Carvalho et al., 2011). Therefore, it is unlikely that the combination of both mutations (*sp* and *dgt*) would be affected epistatically by the *d* allele (Campos et al., 2010). Interestingly, the *dgt* mutation delays the number of days to flowering in both *SP* and *sp* backgrounds (Balbi and Lomax, 2003),

apparently by reducing the expression of the *SFT* gene, which encodes the florigen (Evans, 1971; Shalit et al., 2009). It does not, however, significantly affect the number of leaves produced before termination, which is a proven effect of *SFT* and its orthologs in tomato and other species (Kojima et al., 2002; Lifschitz and Eshed, 2006; Navarro et al., 2015). Hence, the loss-of-function *sft* mutant produced 130% more leaves on the primary shoot than the control cv MT (Vicente et al., 2015). Conversely, transgenic tomato plants overexpressing *SFT* flower after producing only three or four leaves (Molinero-Rosales et al., 2004; Shalit et al., 2009).

Axillary branching was increased in *sp* mutants in both *DGT* and *dgt* allele backgrounds. The expression of *SP* is higher in axillary meristems, suggesting a possible role for *SP* in the control of apical dominance (Thouet et al., 2008). Our results reinforce this notion, as *sp* mutants are more profusely branched than wild-type plants. This also agrees with the effects of the *SP* ortholog *Dt1* in soybean, where comparison of determinate and indeterminate isogenic lines revealed an increased propensity to side branching in the former (Gai et al., 1984). The *dgt* mutant responds to auxin treatment of decapitated shoots, which inhibits bud outgrowth to the same extent as in wild-type plants (Cline, 1994). Apical dominance has been reported to be reduced in intact *dgt* plants (Coenen et al., 2003), but caution should be exercised when interpreting these results, as published work on *dgt* has been conducted in tomato cultivars differing in their *SP* alleles (Supplemental Table S1). Our results indicate a strong and complex interaction between *SP* and *DGT* in the control of apical dominance: the *dgt* mutation increased it in the wild-type *SP* background but also increased axillary bud outgrowth in the *sp* background, enhancing its branching phenotype.

Control of Endogenous Auxin Levels and PAT by SP and DGT

Endogenous IAA concentration and distribution within tissues determine a wide range of plant developmental processes, including apical dominance, stem growth, vascular patterning, root development, and others (Petrášek and Friml, 2009; Ljung, 2013). IAA synthesis is maximal in younger, developing parts of the plant such as leaflets and root apices (Ljung et al., 2001). IAA levels in dark-grown seedlings (Fujino et al., 1988) and roots (Muday et al., 1995) of *sp dgt* and *SP DGT* plants are indistinguishable. However, free IAA levels in aerial parts of 7-d-old light-grown seedlings of *sp dgt* plants were twice as high as in *SP DGT* plants (Fig. 2), suggesting a light-dependent, synergistic influence of the *sp* and *dgt* alleles on auxin synthesis, degradation, or transport.

The above results could reflect changes in IAA biosynthesis, degradation, or transport. The reduction in PAT produced by the *dgt* mutation was described previously (Ivanchenko et al., 2015), but the synergistic effect of the *sp* mutation described here was unexpected. The differences in IAA concentration in the aerial part of the seedlings could be due to altered PAT caused by both the *sp* and *dgt* mutations. PAT from the shoot organs to the root tips induces the formation of the entire plant vascular system (Aloni, 2013; Marcos and Berleth, 2014), as evidenced by the repression of protoxylem formation upon treatment with the auxin transport inhibitor NPA (Bishopp et al., 2011) and the polar localization of PIN1 in preprocambial cells (Scarpella et al., 2006). A lack of large secondary xylem vessels was conspicuous in the *dgt* mutant, as described previously (Zobel, 1974). In plants harboring the functional *DGT* allele, the *sp* mutation led to larger (greater than 800 μm^2 cross-sectional area) vessels compared with wild-type *SP* plants. In tree species, there is evidence that the relationship between xylem vessel density and size involves differential regulation of the duration of tracheid expansion along the longitudinal (Anfodillo et al., 2012; Sorce et al., 2013) and radial (Tuominen et al., 1997) axes. Tree stature has a strong influence on vessel width due to an allometric scaling effect (Morris et al., 2018). It remains to be seen if this also is the case in herbs and if the effect of the *SP* gene on xylem width is caused indirectly by its control of plant height or directly by its influence on PAT. Increased PAT in the *polycotyledon* tomato mutant, for instance, leads to an altered vascular pattern in the hypocotyl (Al-Hammadi et al., 2003; Kharshiing et al., 2010).

SP Affects Excised Hypocotyl Elongation, Gravitropic Responses, and Root Regeneration and Elongation

The elongation of excised hypocotyl segments in response to different concentrations of exogenous auxin is a classical assay for auxin sensitivity (Gendreau et al., 1997; Collett et al., 2000). The hypocotyl elongation response of *dgt* has been described in the background of tomato cv VFN8, a mutant for *sp* (Supplemental Table S1). In both intact or excised hypocotyl segments, a reduced response to exogenous auxin was observed for the *sp dgt* double mutant (Kelly and Bradford, 1986; Rice and Lomax, 2000). We confirmed these results but show that a functional *SP* allele leads to increased elongation in either the *DGT* or *dgt* background. Collectively, these results indicate that some compensatory effect can be ascribed to SP in this response. Hypocotyl elongation in Arabidopsis relies on auxin-induced changes in the activity of plasma membrane H^+-ATPases, which leads to increased H^+ extrusion and cell expansion, through expansin-mediated cell wall loosening, according to the acid growth theory (Takahashi et al., 2012). Hypocotyl elongation upon exogenous auxin application points to a positive effect of SP on the activity of plasma membrane H^+-ATPases. Interestingly, the activity of both plasma membrane H^+-ATPases and PIN efflux transporters, which also are influenced by SP at the transcriptional level (Fig. 4), is regulated by changes in their phosphorylation state (Takahashi et al.,

2012; Zourelidou et al., 2014; Weller et al., 2017). This fits with earlier suggestions that *SP*, which encodes a PEBP, exerts at least some of its effects on membrane proteins through interaction with kinases (Pnueli et al., 2001).

The Cholodny-Went hypothesis is a classical model suggesting that differential auxin distribution is the cause of directional plant bending with respect to an exogenous stimulus such as light or gravity (Went, 1974). DGT is required for a correct gravitropic response of roots and shoots, but the explanation at the molecular level is still lacking (Muday et al., 1995; Rice and Lomax, 2000). Functional SP enhances shoot gravitropism in horizontally positioned plants of either the *DGT* or *dgt* background. Functional SP produces taller plants, so it is tempting to speculate that they should have a stronger gravitropic response to facilitate the bending of a larger stem. In Arabidopsis, the IAA efflux transporter PIN3 mediates the lateral redistribution of auxin and, therefore, is involved in hypocotyl and root tropisms (Friml et al., 2002). It seems reasonable to suggest a link between SP and PIN3 in the face of our *PIN* gene expression profiles (Fig. 5). Remarkably, both types of efflux transporters, PIN1 and PIN3, have been shown to relocate at the subcellular level via the same mechanism: vesicle trafficking along the actin cytoskeleton between the plasma membrane and endosomes (Geldner et al., 2001; Friml et al., 2002). Dissecting the intertwined mechanisms involved in this possible coregulation will be required to fully understand the extent to which and exactly how SP affects auxin distribution.

High concentrations of exogenous auxin inhibit root elongation. As expected, the *dgt* mutation reduced auxin-induced inhibition (Coenen and Lomax, 1998) in root elongation; however, a functional *SP* allele led to lower inhibition than in the double *sp dgt* mutant. This result could be ascribed to a new balance in auxin transport and signaling produced by the combination of *SP* and *DGT*. Root growth increases with the strength of auxin signaling up to a certain optimum and then begins to decline, probably following a parabolic trajectory (Sibout et al., 2006). In vitro root regeneration, on the other hand, is stimulated by low concentrations of auxin, and *dgt* is relatively insensitive to this exogenous treatment (Coenen and Lomax, 1998). Interestingly, the *sp* mutation also reduces rhizogenesis (Supplemental Fig. S3), which reinforces the notion of *SP* positively influencing PAT, as the PAT inhibitor 2,3,5-triiodobenzoic acid has been shown to reduce in vitro root formation in tomato (Tyburski and Tretyn, 2004).

Interactions between SP and the Auxin Signaling Machinery

Auxin signaling output can be estimated by following the pattern of *DR5* promoter activation (Ulmasov et al., 1995; Liao et al., 2015). For example, GUS staining of *DR5*::*GUS* revealed that auxin flux at the root tips proceeds acropetally up to the root cap, where it is redistributed via lateral efflux transporters toward a peripheral basipetal transport route (Benková et al., 2003; Paciorek et al., 2005). Exogenous auxin application leads to greater GUS signal in seedlings with a functional *SP* allele, probably owing to alterations in the auxin signaling machinery produced by SP, such as the expression of *Aux/IAA* and *ARF* family genes (Fig. 6).

Auxin signaling is strongly dependent on auxin levels and the responsiveness of target cells. At low IAA levels, a suite of repressor proteins, including Aux/IAA and TOPLESS, repress ARFs, a group of transcription factors that regulate the expression of auxin-responsive genes (Causier et al., 2012; Bargmann and Estelle, 2014; Chandler, 2016). At high IAA levels, auxin acts as a molecular glue to stabilize the TIR1/AFB receptor binding and tagging of Aux/IAAs for 26S proteasome degradation (Hayashi, 2012). This, in turn, frees ARFs bound to AuxRE in the genome (TGTCTC or its degenerate, but also functional, form, TGTCNC) to activate or repress gene expression (Ulmasov et al., 1995). Our in silico analyses demonstrated the presence of conserved AuxRE elements both 5′ (upstream) and 3′ (downstream) of the *SP* coding sequence in the genome of tomato and closely related species. The 3′ region of *TFL1* in Arabidopsis contains multiple auxin cis-regulatory elements key for the control of spatiotemporal expression of the gene (Serrano-Mislata et al., 2016). It remains to be determined whether such cis-regulatory elements also are functional in tomato and if they are involved in the response of *SP* expression to auxin.

Tomato has 25 *Aux/IAA* and 22 *ARF* genes (Audran-Delalande et al., 2012; Zouine et al., 2014), indicating that auxin signaling is very complex. DGT can alter the expression of genes related to auxin signaling (Mito and Bennett, 1995), including *Aux/IAA* genes (Nebenführ et al., 2000). PPIases catalyze the cis/trans-isomerization of peptide bonds preceding Pro residues of target peptides, including Aux/IAAs (Jing et al., 2015). Only Aux/IAA peptides of the right conformation can bind to the TIR1 receptor and be tagged for degradation, and PPIases, such as DGT, are believed to play a key role in auxin perception (Su et al., 2015). It is likely that some transcriptional feedback exists when the right conformers are not produced, as suggested by the increased transcript levels of *IAA3* and the reduced levels of *IAA9* in *dgt* mutants. Furthermore, our in silico analysis shows that the *sp* mutation occurs in a highly conserved cis-Pro residue in a DPDxPxn10H consensus region in the PEBP domain (Supplemental Fig. S5), which is a potential target for PPIases. Whether this putative molecular interaction between SP and DGT could account for the phenotypic outcomes shown here remains to be determined.

CONCLUSION

Auxin gradients are critical for organogenesis in the shoot apex; however, the influence of this hormone on

shoot determinacy, which is a key determinant of growth habit, remains unclear. Our data link auxin and the antiflorigenic protein SP, the main switch between indeterminate and determinate growth habits in tomato. Although it is not clear whether auxin itself can affect growth habit, a physiological interaction between this hormone and members of the CETS family was clearly demonstrated here. Hence, *SP* alleles affected various auxin-related responses (e.g. apical dominance, PIN1-mediated PAT, vascular differentiation, H^+ extrusion, and gravitropism responses), different *SP* orthologs presented AuxREs, and the auxin mutant *dgt* down-regulated *SFT* and up-regulated *SP* expression. Increasing evidence shows that the *SP*/*SFT* genetic module is a hub in crop productivity, affecting heterosis for yield (Krieger et al., 2010) and improving plant architecture and the vegetative-to-reproductive balance (McGarry and Ayre, 2012; Vicente et al., 2015; Zsögön et al., 2017). Our results suggest that at least part of the effect of the SP/SFT module on yield is mediated by auxin. This knowledge may inspire novel and more precise manipulation of this hormone for applications in agriculture.

MATERIALS AND METHODS

Plant Material

Seeds of tomato (*Solanum lycopersicum* 'MT') were donated by Dr. Avram Levy (Weizmann Institute of Science) in 1998 and subsequently maintained (through self-pollination) as a true-to-type cultivar. The cv MT seeds carrying the synthetic auxin-responsive (*DR5*) promoter fused to the reporter gene *uid* (encoding a GUS) were obtained from Dr. José Luiz García-Martínez (Universidad Politécnica de Valencia). The *dgt* mutation was introgressed into cv MT from its original background in cv VFN8 (LA1529), donated by Dr. Roger Chetelat (Tomato Genetics Resource Center, University of California, Davis). The functional allele of *SP* was introgressed from cv Moneymaker (LA2706).

The introgression of mutations into cv MT was described previously (Carvalho et al., 2011). A comparison between indeterminate (*SP/SP*) and determinate (*sp/sp*) plants in the cv MT background has been published previously (Vicente et al., 2015). Both *sp* and *dgt* mutations were confirmed by cleaved-amplified polymorphic sequence (CAPS) marker analyses and sequencing. All experiments were conducted on BC_6F_3 plants or subsequent generations (Sestari et al., 2014). In vitro seedling cultivation was conducted under controlled conditions (16-h/8-h day/night, approximately 45 μmol m^{-2} s^{-1} photosynthetically active radiation, and 25°C ± 1°C) in flasks with 30 mL of half-strength Murashige-Skoog medium gellified with 0.5% (w/v) agar, pH 5.8. Seeds were surface sterilized by agitation in 30% (v/v) commercial bleach (2.7% [w/v] sodium hypochlorite) for 15 min followed by three rinses with sterile distilled water.

Growth Conditions

Plants were grown in a greenhouse in Viçosa (642 m above sea level, 20°45′S, 42°51′W), Minas Gerais, Brazil, under semicontrolled conditions: mean temperature of 28°C, 11.5-h/13-h (winter/summer) photoperiod, 250 to 350 μmol m^{-2} s^{-1} PAR, and irrigation to field capacity twice per day. Seeds were germinated in 350-mL pots with a 1:1 (v/v) mixture of commercial potting mix (Basaplan; Base Agro) and expanded vermiculite supplemented with 1 g L^{-1} 10:10:10 NPK and 4 g L^{-1} dolomite limestone ($MgCO_3$ + $CaCO_3$). Upon appearance of the first true leaf, seedlings of each genotype were transplanted to pots containing the soil mix described above, except for the NPK supplementation, which was increased to 8 g L^{-1}.

Auxin Quantification

Endogenous IAA levels were determined by gas chromatography-tandem mass spectrometry-selecting ion monitoring (Shimadzu model GCMS-QP2010 SE). Samples (50–100 mg fresh weight) were extracted and methylated as described (Rigui et al., 2015). About 0.25 μg of the labeled standard [$^{13}C_6$]IAA (Cambridge Isotopes) was added to each sample as an internal standard. The chromatograph was equipped with a fused-silica capillary column (30 m i.d., 0.25 mm, 0.5-μm-thick internal film) DB-5 MS stationary phase using helium as the carrier gas at a flow rate of 4.5 mL min^{-1} in the following program: 2 min at 100°C, followed by a ramp of 10°C min^{-1} to 140°C, 25°C min^{-1} to 160°C, 35°C min^{-1} to 250°C, 20°C min^{-1} to 270°C, and 30°C min^{-1} to 300°C. The injector temperature was 250°C, and the following mass spectrometer operating parameters were used: ionization voltage, 70 eV (electron impact ionization); ion source temperature, 230°C; and interface temperature, 260°C. Ions with mass-to-charge ratios of 130 and 189 (corresponding to endogenous IAA) and 136 and 195 (corresponding to [$^{13}C_6$]IAA) were monitored, and endogenous IAA concentrations were calculated based on extracted chromatograms at mass-to-charge ratios of 130 and 136.

PAT Analysis

PAT was assayed in hypocotyl segments of 2-week-old seedlings according to the protocol originally described by Al-Hammadi et al. (2003), with some modifications. Briefly, 10-mm hypocotyl sections were excised and incubated in 5 mM phosphate buffer (pH 5.8) containing 1 μM IAA for 2 h at 25°C ± 2°C on a rotary shaker (200 rpm). These segments were placed between receiver blocks (1% [w/v] agar in water) and donor blocks (1% [w/v] agar in 5 mM phosphate buffer [pH 5.8] containing 1 μM IAA and 100 nM [^{3}H]IAA) oriented with their apical ends toward the donor blocks. After 4 h of incubation inside a humid chamber at 25°C ± 2°C, the receiver blocks were removed and stored in a 3-mL scintillation cocktail (Ultima Gold; PerkinElmer). Receiver blocks plus scintillation cocktail were shaken overnight at 100 rpm and 28°C ± 2°C before analysis in a scintillation counter. As a negative control, some hypocotyl segments were sandwiched for 30 min between NPA-containing blocks (1% [w/v] agar in water containing 20 μM NPA) prior to the auxin transport assays. ^{3}H dpm was converted to fmol of auxin transported as described by Lewis and Muday (2009).

Auxin Sensitivity Assays

Root regeneration from cotyledon explants was conducted as described previously (Cary et al., 2001). Briefly, cotyledon explants were obtained from 8-d-old seedlings germinated in vitro in one-half-strength MS medium. The explants were then incubated on petri dishes containing MS medium with or without supplementation with 0.4 μM NAA. After 8 d, the number of explants with visible roots (determined using a magnifying glass) was counted.

For hypocotyl elongation assays, hypocotyls were excised from 2-week-old seedlings and cut into 5-mm sections. Between 15 and 20 segments were preincubated for each treatment and floated on buffer (10 mM KCl, 1 mM MES-KOH [pH 6], and 1% [w/v] Suc) for 2 h at 25°C in the dark to deplete endogenous auxin. Segments were then incubated on buffer (10 mM KCl, 1 mM MES-KOH [pH 6], 1%[w/v] Suc, and 0.4 μM NAA) for 24 h on a shaker at 25°C under white light. Segments were photographed to determine their length using ImageJ (NIH). The experiment was repeated three times with similar results.

For the gravitropism assays, plants were germinated in 350-mL pots and transferred to 50-mL Falcon tubes for 2 dag. The gravitropic response was assessed at 10 dag by placing five plants of each genotype horizontally and photographing them in 30-min intervals. The angle of shoot bending at each time point was determined using AutoCad 2016 (Autodesk). Sterilized seeds were germinated in petri dishes onto two layers of filter paper moistened with distilled water and incubated for 4 d at 25°C in the dark. Ten germinated seeds with radicles of 5 to 10 mm were transferred to vertically oriented square petri dishes (120 mm × 120 mm) aligned on each plate with the radicles pointing down. The plates contained MS medium supplemented with vitamins, pH 5.7, 3% (w/v) Suc, 0.8% (w/v) agar, and 10 μM NAA for the auxin treatment. Plates were incubated in a growth chamber in the dark.

In vitro root elongation in response to exogenous auxin was assessed as follows. Seeds were surface sterilized and imbibed for 2 d at 4°C in the dark on agar plates containing one-half-strength MS growth medium (Murashige and Skoog, 1962) and then transferred to a growth chamber under control conditions (12-h photoperiod, 150 μmol m^{-2} s^{-1} white light, 22°C/20°C throughout the day/night cycle, and 60% relative humidity). After 4 d, 10 seedlings per plate were transferred to one-half-strength MS medium with or without 10 μM NAA (Sigma-Aldrich) and covered completely with aluminum foil for 8 d. Root elongation was assessed every 2 d under dim light conditions.

Histochemical Assays

Transgenic *DR5*::*GUS* plants were incubated overnight at 37°C in GUS staining solution [100 mM NaH_2PO_4, 10 mM EDTA, 0.5 mM $K_4Fe(CN)_6$, 0.05% v/v Triton X-100, and 1 mM 5-bromo-4-chloro-3-indolyl-β-D-GlcA]. Following GUS staining, samples were washed in a graded ethanol series to remove chlorophyll. Samples were then photographed using a Leica S8AP0 microscope set to 80× magnification coupled to a Leica DFC295 camera. Quantitative GUS activity was assayed according to Jefferson et al. (1987) with some modifications. Briefly, samples were ground in liquid nitrogen and subsequently homogenized in MUG extraction buffer composed of 50 mM HEPES-KOH (pH 7), 5 mM DTT, and 0.5% (w/v) polyvinylpyrrolidone. After centrifugation, 200-μL aliquots of the supernatant were mixed with 200 μL of GUS assay buffer composed of 50 mM HEPES-KOH (pH 7), 5 mM DTT, 10 mM EDTA, and 2 mM 4-methylumbelliferyl-β-D-glucuronide (MUG) and incubated at 37°C for 30 min. Subsequently, aliquots of 100 μL were taken from each tube, and the reactions were stopped and fluorescence was analyzed using a spectrofluorometer (LS55; PerkinElmer) with 365-nm excitation and 460-nm emission wavelengths (5-nm bandwidth).

Gene Expression Analyses

Total RNA was extracted from approximately 30 mg fresh weight of sympodial meristems of 10-d-old plants following the protocol of the manufacturer (Promega SV total RNA isolation system). For auxin treatments, plants were sprayed previously with 10 μM IAA or mock sprayed 24 h prior to RNA extraction. Four biological replicates were used for subsequent cDNA synthesis, where each replicate consisted of a pool of three plants. Each replicate was used for the analyses, since sympodial meristems are small and did not provide enough biological material for RNA extraction. Two technical replicates were then performed on each of the four samples. RNA integrity was analyzed on a 1% w/v agarose gel, and RNA concentration was estimated before and after treatment with DNase I (Amplification Grade DNase I; Invitrogen). Total RNA was transcribed into cDNA using the enzyme reverse transcriptase and the Universal RiboClone cDNA Synthesis System (Promega), following the manufacturer's protocols.

For gene expression analyses, Power SYBR Green PCR Master Mix was used on MicroAmp Optical 96-well reaction plates (both from Applied Biosystems) and MicroAmp Optical adhesive film (Applied Biosystems). The number of reactions from the cycle threshold (CT) as well as the efficiency of the reaction were estimated using the Real-Time PCR Miner tool (Zhao and Fernald, 2005).

Relative expression was normalized using *ACTIN* and *UBIQUITIN*; *ACTIN* was used to calculate ΔΔCT assuming 100% efficiency of amplification of genes ($2^{-\Delta\Delta CT}$). Primer sequences used are shown in Supplemental Table S2. Melting curves were checked for unspecific amplifications and primer dimerization.

In Silico Sequence Analyses

SP gene alignments was performed using the ClustalW alignment option of the Geneious R9 (Biomatters) software package.

Statistical Analysis

ANOVA and Tukey's honestly significant difference test were performed using Assistat 7.6 beta (http://assistat.com). Percentage data were converted to inverse function (1/X) before analysis.

Accession Numbers

Gene accession numbers are as follows: JN379431 (*IAA1*), JN379432 (*IAA2*), JN379433 (*IAA3*), JN379437 (*IAA9*), EF667342 (*ARF8*), JF911788 (*ARF10*), U84140 (*SP*), AY186735 (*SFT*), HQ127074 (*PIN1*), HQ127077 (*PIN2*), HQ127079 (*PIN3*), NM_001247559 (*DGT*), NM_001308447 (*ACTIN*), and X58253 (*UBIQUITIN*).

Supplemental Data

The following supplemental materials are available.

Supplemental Figure S1. The rate of meristem maturation is affected by the combination of *SP* and *DGT* alleles.

Supplemental Figure S2. The effects of SP on flowering are not dependent on brassinosteroid biosynthesis.

Supplemental Figure S3. Impact of the *sp* mutation on in vitro root regeneration.

Supplemental Figure S4. Expression pattern of the GUS reporter driven by the auxin-inducible *DR5* promoter in the *sp dgt* double mutant.

Supplemental Figure S5. The tomato *sp* mutation occurs in a highly conserved Pro residue.

Supplemental Table S1. List of publications featuring the tomato *dgt* mutant.

Supplemental Table S2. Primers used for quantitative PCR analyses in this work.

Received January 23, 2018; accepted February 22, 2018; published March 2, 2018.

LITERATURE CITED

Al-Hammadi ASAA, Sreelakshmi Y, Negi S, Siddiqi I, Sharma R (2003) The polycotyledon mutant of tomato shows enhanced polar auxin transport. Plant Physiol **133:** 113–125

Aloni R (2013) Role of hormones in controlling vascular differentiation and the mechanism of lateral root initiation. Planta **238:** 819–830

Alvarez J, Guli CL, Yu XH, Smyth DR (1992) Terminal flower: a gene affecting inflorescence development in Arabidopsis thaliana. Plant J **2:** 103–116

Anfodillo T, Deslauriers A, Menardi R, Tedoldi L, Petit G, Rossi S (2012) Widening of xylem conduits in a conifer tree depends on the longer time of cell expansion downwards along the stem. J Exp Bot **63:** 837–845

Audran-Delalande C, Bassa C, Mila I, Regad F, Zouine M, Bouzayen M (2012) Genome-wide identification, functional analysis and expression profiling of the Aux/IAA gene family in tomato. Plant Cell Physiol **53:** 659–672

Balbi V, Lomax TL (2003) Regulation of early tomato fruit development by the *Diageotropica* gene. Plant Physiol **131:** 186–197

Bargmann BOR, Estelle M (2014) Auxin perception: in the IAA of the beholder. Physiol Plant **151:** 52–61

Bartel B, Fink GR (1995) ILR1, an amidohydrolase that releases active indole-3-acetic acid from conjugates. Science **268:** 1745–1748

Benková E, Michniewicz M, Sauer M, Teichmann T, Seifertová D, Jürgens G, Friml J (2003) Local, efflux-dependent auxin gradients as a common module for plant organ formation. Cell **115:** 591–602

Berleth T, Sachs T (2001) Plant morphogenesis: long-distance coordination and local patterning. Curr Opin Plant Biol **4:** 57–62

Bishop GJ, Nomura T, Yokota T, Harrison K, Noguchi T, Fujioka S, Takatsuto S, Jones JDG, Kamiya Y (1999) The tomato DWARF enzyme catalyses C-6 oxidation in brassinosteroid biosynthesis. Proc Natl Acad Sci USA **96:** 1761–1766

Bishopp A, Help H, El-Showk S, Weijers D, Scheres B, Friml J, Benková E, Mähönen AP, Helariutta Y (2011) A mutually inhibitory interaction between auxin and cytokinin specifies vascular pattern in roots. Curr Biol **21:** 917–926

Blilou I, Xu J, Wildwater M, Willemsen V, Paponov I, Friml J, Heidstra R, Aida M, Palme K, Scheres B (2005) The PIN auxin efflux facilitator network controls growth and patterning in Arabidopsis roots. Nature **433:** 39–44

Bradley D, Carpenter R, Copsey L, Vincent C, Rothstein S, Coen E (1996) Control of inflorescence architecture in Antirrhinum. Nature **379:** 791–797

Campos ML, Carvalho RF, Benedito VA, Peres LEP (2010) Small and remarkable: the Micro-Tom model system as a tool to discover novel hormonal functions and interactions. Plant Signal Behav **5:** 267–270

Carvalho RF, Campos ML, Pino LE, Crestana SL, Zsögön A, Lima JE, Benedito VA, Peres LEP (2011) Convergence of developmental mutants into a single tomato model system: 'Micro-Tom' as an effective toolkit for plant development research. Plant Methods **7:** 18

Cary A, Uttamchandani SJ, Smets R, Van Onckelen HA, Howell SH (2001) Arabidopsis mutants with increased organ regeneration in tissue

culture are more competent to respond to hormonal signals. Planta **213:** 700–707

Causier B, Lloyd J, Stevens L, Davies B (2012) TOPLESS co-repressor interactions and their evolutionary conservation in plants. Plant Signal Behav **7:** 325–328

Chandler JW (2016) Auxin response factors. Plant Cell Environ **39:** 1014–1028

Cline MG (1994) The role of hormones in apical dominance: new approaches to an old problem in plant development. Physiol Plant **90:** 230–237

Coenen C, Christian M, Lüthen H, Lomax TL (2003) Cytokinin inhibits a subset of diageotropica-dependent primary auxin responses in tomato. Plant Physiol **131:** 1692–1704

Coenen C, Lomax TL (1998) The *diageotropica* gene differentially affects auxin and cytokinin responses throughout development in tomato. Plant Physiol **117:** 63–72

Collett CE, Harberd NP, Leyser O (2000) Hormonal interactions in the control of Arabidopsis hypocotyl elongation. Plant Physiol **124:** 553–562

Domagalska MA, Sarnowska E, Nagy F, Davis SJ (2010) Genetic analyses of interactions among gibberellin, abscisic acid, and brassinosteroids in the control of flowering time in Arabidopsis thaliana. PLoS ONE **5:** e14012

Evans LT (1971) Flower induction and the florigen concept. Annu Rev Plant Physiol **22:** 365–394

Friml J (2003) Auxin transport: shaping the plant. Curr Opin Plant Biol **6:** 7–12

Friml J, Benfey P, Benková E, Bennett M, Berleth T, Geldner N, Grebe M, Heisler M, Hejátko J, Jürgens G, et al (2006) Apical-basal polarity: why plant cells don't stand on their heads. Trends Plant Sci **11:** 12–14

Friml J, Wiśniewska J, Benková E, Mendgen K, Palme K (2002) Lateral relocation of auxin efflux regulator PIN3 mediates tropism in Arabidopsis. Nature **415:** 806–809

Fujino DW, Nissen SJ, Jones AD, Burger DW, Bradford KJ (1988) Quantification of indole-3-acetic acid in dark-grown seedlings of the *diageotropica* and epinastic mutants of tomato (*Lycopersicon esculentum* Mill.). Plant Physiol **88:** 780–784

Gai J, Palmer RG, Fehr WR (1984) Bloom and pod set in determinate and indeterminate soybeans grown in China. Agron J **76:** 979

Geldner N, Friml J, Stierhof YD, Jürgens G, Palme K (2001) Auxin transport inhibitors block PIN1 cycling and vesicle trafficking. Nature **413:** 425–428

Gendreau E, Traas J, Desnos T, Grandjean O, Caboche M, Höfte H (1997) Cellular basis of hypocotyl growth in *Arabidopsis thaliana*. Plant Physiol **114:** 295–305

Hayashi K (2012) The interaction and integration of auxin signaling components. Plant Cell Physiol **53:** 965–975

Hengst U, Albrecht H, Hess D, Monard D (2001) The phosphatidylethanolamine-binding protein is the prototype of a novel family of serine protease inhibitors. J Biol Chem **276:** 535–540

Ivanchenko MG, Zhu J, Wang B, Medvecká E, Du Y, Azzarello E, Mancuso S, Megraw M, Filichkin S, Dubrovsky JG, et al (2015) The cyclophilin A DIAGEOTROPICA gene affects auxin transport in both root and shoot to control lateral root formation. Development **142:** 712–721

Jefferson RA, Kavanagh TA, Bevan MW (1987) GUS fusions: beta-glucuronidase as a sensitive and versatile gene fusion marker in higher plants. EMBO J **6:** 3901–3907

Jing H, Yang X, Zhang J, Liu X, Zheng H, Dong G, Nian J, Feng J, Xia B, Qian Q, et al (2015) Peptidyl-prolyl isomerization targets rice Aux/IAAs for proteasomal degradation during auxin signalling. Nat Commun **6:** 7395

Kelly MO, Bradford KJ (1986) Insensitivity of the *diageotropica* tomato mutant to auxin. Plant Physiol **82:** 713–717

Kharshiing EV, Kumar GP, Ditengou FA, Li X, Palme K, Sharma R (2010) The *polycotyledon* (*pct1-2*) mutant of tomato shows enhanced accumulation of PIN1 auxin transport facilitator protein. Plant Biol (Stuttg) **12:** 224–228

Kojima S, Takahashi Y, Kobayashi Y, Monna L, Sasaki T, Araki T, Yano M (2002) Hd3a, a rice ortholog of the Arabidopsis FT gene, promotes transition to flowering downstream of Hd1 under short-day conditions. Plant Cell Physiol **43:** 1096–1105

Krieger U, Lippman ZB, Zamir D (2010) The flowering gene SINGLE FLOWER TRUSS drives heterosis for yield in tomato. Nat Genet **42:** 459–463

Kroslak T, Koch T, Kahl E, Höllt V (2001) Human phosphatidylethanolamine-binding protein facilitates heterotrimeric G protein-dependent signaling. J Biol Chem **276:** 39772–39778

Kumari S, Roy S, Singh P, Singla-Pareek SL, Pareek A (2013) Cyclophilins: proteins in search of function. Plant Signal Behav **8:** e22734

Lavy M, Prigge MJ, Tigyi K, Estelle M (2012) The cyclophilin DIAGEOTROPICA has a conserved role in auxin signaling. Development **139:** 1115–1124

Lewis DR, Muday GK (2009) Measurement of auxin transport in Arabidopsis thaliana. Nat Protoc **4:** 437–451

Li J, Li Y, Chen S, An L (2010) Involvement of brassinosteroid signals in the floral-induction network of Arabidopsis. J Exp Bot **61:** 4221–4230

Liao CY, Smet W, Brunoud G, Yoshida S, Vernoux T, Weijers D (2015) Reporters for sensitive and quantitative measurement of auxin response. Nat Methods **12:** 207–210

Lifschitz E, Eshed Y (2006) Universal florigenic signals triggered by FT homologues regulate growth and flowering cycles in perennial day-neutral tomato. J Exp Bot **57:** 3405–3414

Ljung K (2013) Auxin metabolism and homeostasis during plant development. Development **140:** 943–950

Ljung K, Bhalerao RP, Sandberg G (2001) Sites and homeostatic control of auxin biosynthesis in Arabidopsis during vegetative growth. Plant J **28:** 465–474

MacArthur JW (1934) Linkage groups in the tomato. J Genet **29:** 123–133

Marcos D, Berleth T (2014) Dynamic auxin transport patterns preceding vein formation revealed by live-imaging of Arabidopsis leaf primordia. Front Plant Sci **5:** 235

Martí E, Gisbert C, Bishop GJ, Dixon MS, García-Martínez JL (2006) Genetic and physiological characterization of tomato cv. Micro-Tom. J Exp Bot **57:** 2037–2047

McGarry RC, Ayre BG (2012) Manipulating plant architecture with members of the CETS gene family. Plant Sci **188-189:** 71–81

Mito N, Bennett AB (1995) The diageotropica mutation and synthetic auxins differentially affect the expression of auxin-regulated genes in tomato. Plant Physiol **109:** 293–297

Molinero-Rosales N, Latorre A, Jamilena M, Lozano R (2004) SINGLE FLOWER TRUSS regulates the transition and maintenance of flowering in tomato. Planta **218:** 427–434

Morita MT (2010) Directional gravity sensing in gravitropism. Annu Rev Plant Biol **61:** 705–720

Morris H, Gillingham MAF, Plavcová L, Gleason SM, Olson ME, Coomes DA, Fichtler E, Klepsch MM, Martínez-Cabrera HI, McGlinn DJ, et al (2018) Vessel diameter is related to amount and spatial arrangement of axial parenchyma in woody angiosperms. Plant Cell Environ **41:** 245–260

Muday GK, Lomax TL, Rayle DL (1995) Characterization of the growth and auxin physiology of roots of the tomato mutant, diageotropica. Planta **195:** 548–553

Murashige T, Skoog F (1962) A revised medium for rapid growth and bio assays with tobacco tissue cultures. Physiol Plant **15:** 473–497

Navarro C, Cruz-Oró E, Prat S (2015) Conserved function of FLOWERING LOCUS T (FT) homologues as signals for storage organ differentiation. Curr Opin Plant Biol **23:** 45–53

Nebenführ A, White TJ, Lomax TL (2000) The diageotropica mutation alters auxin induction of a subset of the Aux/IAA gene family in tomato. Plant Mol Biol **44:** 73–84

Oh K, Ivanchenko MG, White TJ, Lomax TL (2006) The diageotropica gene of tomato encodes a cyclophilin: a novel player in auxin signaling. Planta **224:** 133–144

Ouattara S, Weaver DB (1994) Effect of growth habit on yield and agronomic characteristics of late-planted soybean. Crop Sci **34:** 870

Paciorek T, Zazímalová E, Ruthardt N, Petrásek J, Stierhof YD, Kleine-Vehn J, Morris DA, Emans N, Jürgens G, Geldner N, et al (2005) Auxin inhibits endocytosis and promotes its own efflux from cells. Nature **435:** 1251–1256

Park SJ, Eshed Y, Lippman ZB (2014) Meristem maturation and inflorescence architecture: lessons from the Solanaceae. Curr Opin Plant Biol **17:** 70–77

Petrášek J, Friml J (2009) Auxin transport routes in plant development. Development **136:** 2675–2688

Pnueli L, Carmel-Goren L, Hareven D, Gutfinger T, Alvarez J, Ganal M, Zamir D, Lifschitz E (1998) The SELF-PRUNING gene of tomato regulates vegetative to reproductive switching of sympodial meristems and is the ortholog of CEN and TFL1. Development **125:** 1979–1989

Pnueli L, Gutfinger T, Hareven D, Ben-Naim O, Ron N, Adir N, Lifschitz E (2001) Tomato SP-interacting proteins define a conserved signaling system that regulates shoot architecture and flowering. Plant Cell **13:** 2687–2702

Ratcliffe OJ, Amaya I, Vincent CA, Rothstein S, Carpenter R, Coen ES, Bradley DJ (1998) A common mechanism controls the life cycle and architecture of plants. Development **125:** 1609–1615

Reinhardt D, Pesce ER, Stieger P, Mandel T, Baltensperger K, Bennett M, Traas J, Friml J, Kuhlemeier C (2003) Regulation of phyllotaxis by polar auxin transport. Nature **426:** 255–260

Repinski SL, Kwak M, Gepts P (2012) The common bean growth habit gene PvTFL1y is a functional homolog of Arabidopsis TFL1. Theor Appl Genet **124:** 1539–1547

Rice MS, Lomax TL (2000) The auxin-resistant *diageotropica* mutant of tomato responds to gravity via an auxin-mediated pathway. Planta **210:** 906–913

Rick CM (1978) The tomato. Sci Am **239:** 76–87

Rigui AP, Gaspar M, Oliveira VF, Purgatto E, Carvalho MA (2015) Endogenous hormone concentrations correlate with fructan metabolism throughout the phenological cycle in *Chrysolaena obovata*. Ann Bot **115:** 1163–1175

Rubery PH, Sheldrake AR (1974) Carrier-mediated auxin transport. Planta **118:** 101–121

Samach A, Lotan H (2007) The transition to flowering in tomato. Plant Biotechnol **24:** 71–82

Scarpella E (2017) The logic of plant vascular patterning: polarity, continuity and plasticity in the formation of the veins and of their networks. Curr Opin Genet Dev **45:** 34–43

Scarpella E, Marcos D, Friml J, Berleth T (2006) Control of leaf vascular patterning by polar auxin transport. Genes Dev **20:** 1015–1027

Serrano-Mislata A, Fernández-Nohales P, Doménech MJ, Hanzawa Y, Bradley D, Madueño F (2016) Separate elements of the TERMINAL FLOWER 1 cis-regulatory region integrate pathways to control flowering time and shoot meristem identity. Development **143:** 3315–3327

Sestari I, Zsögön A, Rehder GG, Teixeira LdL, Hassimotto NMA, Purgatto E, Benedito VA, Peres LEP (2014) Near-isogenic lines enhancing ascorbic acid, anthocyanin and carotenoid content in tomato (*Solanum lycopersicum* L. cv Micro-Tom) as a tool to produce nutrient-rich fruits. Sci Hortic (Amsterdam) **175:** 111–120

Shalit A, Rozman A, Goldshmidt A, Alvarez JP, Bowman JL, Eshed Y, Lifschitz E (2009) The flowering hormone florigen functions as a general systemic regulator of growth and termination. Proc Natl Acad Sci USA **106:** 8392–8397

Sheldrake AR (1974) The polarity of auxin transport in inverted cuttings. New Phytol **73:** 637–642

Sibout R, Sukumar P, Hettiarachchi C, Holm M, Muday GK, Hardtke CS (2006) Opposite root growth phenotypes of hy5 versus hy5 hyh mutants correlate with increased constitutive auxin signaling. PLoS Genet **2:** e202

Sorce C, Giovannelli A, Sebastiani L, Anfodillo T (2013) Hormonal signals involved in the regulation of cambial activity, xylogenesis and vessel patterning in trees. Plant Cell Rep **32:** 885–898

Stevens MA, Rick CM (1986) Genetics and breeding. *In* J Atherton, J Rudich, eds, The Tomato Crop: A Scientific Basis for Improvement. Chapman & Hall, London, pp 35–100

Su SH, Gray WM, Masson PH (2015) Auxin: shape matters. Nat Plants **1:** 15097

Takahashi K, Hayashi K, Kinoshita T (2012) Auxin activates the plasma membrane H^+-ATPase by phosphorylation during hypocotyl elongation in Arabidopsis. Plant Physiol **159:** 632–641

Takahashi N, Hayano T, Suzuki M (1989) Peptidyl-prolyl cis-trans isomerase is the cyclosporin A-binding protein cyclophilin. Nature **337:** 473–475

Thouet J, Quinet M, Ormenese S, Kinet JM, Périlleux C (2008) Revisiting the involvement of *SELF-PRUNING* in the sympodial growth of tomato. Plant Physiol **148:** 61–64

Tian Z, Wang X, Lee R, Li Y, Specht JE, Nelson RL, McClean PE, Qiu L, Ma J (2010) Artificial selection for determinate growth habit in soybean. Proc Natl Acad Sci USA **107:** 8563–8568

Tuominen H, Puech L, Fink S, Sundberg B (1997) A radial concentration gradient of indole-3-acetic acid is related to secondary xylem development in hybrid aspen. Plant Physiol **115:** 577–585

Tyburski J, Tretyn A (2004) The role of light and polar auxin transport in root regeneration from hypocotyls of tomato seedling cuttings. Plant Growth Regul **42:** 39–48

Ulmasov T, Liu ZB, Hagen G, Guilfoyle TJ (1995) Composite structure of auxin response elements. Plant Cell **7:** 1611–1623

Vicente MH, Zsögön A, de Sá AFL, Ribeiro RV, Peres LEP (2015) Semi-determinate growth habit adjusts the vegetative-to-reproductive balance and increases productivity and water-use efficiency in tomato (*Solanum lycopersicum*). J Plant Physiol **177:** 11–19

Wang Y, Li J (2008) Molecular basis of plant architecture. Annu Rev Plant Biol **59:** 253–279

Weller B, Zourelidou M, Frank L, Barbosa ICR, Fastner A, Richter S, Jürgens G, Hammes UZ, Schwechheimer C (2017) Dynamic PIN-FORMED auxin efflux carrier phosphorylation at the plasma membrane controls auxin efflux-dependent growth. Proc Natl Acad Sci USA **114:** E887–E896

Went FW (1974) Reflections and speculations. Annu Rev Plant Physiol **25:** 1–27

Wickland DP, Hanzawa Y (2015) The FLOWERING LOCUS T/TERMINAL FLOWER 1 gene family: functional evolution and molecular mechanisms. Mol Plant **8:** 983–997

Yeager AF (1927) Determinate growth in the tomato. J Hered **18:** 263–265

Zhang J, Song Q, Cregan PB, Nelson RL, Wang X, Wu J, Jiang GL (2015) Genome-wide association study for flowering time, maturity dates and plant height in early maturing soybean (Glycine max) germplasm. BMC Genomics **16:** 217

Zhao S, Fernald RD (2005) Comprehensive algorithm for quantitative real-time polymerase chain reaction. J Comput Biol **12:** 1047–1064

Zobel RW (1973) Some physiological characteristics of the ethylene-requiring tomato mutant diageotropica. Plant Physiol **52:** 385–389

Zobel RW (1974) Control of morphogenesis in the ethylene-requiring tomato mutant, *diageotropica*. Can J Bot **52:** 735–741

Zouine M, Fu Y, Chateigner-Boutin ALL, Mila I, Frasse P, Wang H, Audran C, Roustan JPP, Bouzayen M (2014) Characterization of the tomato ARF gene family uncovers a multi-levels post-transcriptional regulation including alternative splicing. PLoS ONE **9:** e84203

Zourelidou M, Absmanner B, Weller B, Barbosa ICR, Willige BC, Fastner A, Streit V, Port SA, Colcombet J, de la Fuente van Bentem S, et al (2014) Auxin efflux by PIN-FORMED proteins is activated by two different protein kinases, D6 PROTEIN KINASE and PINOID. eLife **3:** e02860

Zsögön A, Cermak T, Voytas D, Peres LEP (2017) Genome editing as a tool to achieve the crop ideotype and de novo domestication of wild relatives: case study in tomato. Plant Sci **256:** 120–130